The Stokes−Einstein Relationship and the Levitation Effect: Size-Dependent Diffusion Maximum in Dense Fluids and Close-Packed Disordered Solids

Pradip Kr. Ghorai[†] **and S. Yashonath***[,‡,§]

Solid State and Structural Chemistry Unit and Center for Condensed Matter Theory, Indian Institute of Science, Bangalore 560012, India

Received: August 16, 2004; In Final Form: December 2, 2004

We report a molecular dynamics study of a binary mixture consisting of a large (host) particle and a smaller (guest) particle whose radius is varied over a range. These simulations investigate the possible existence of a diffusion anomaly or levitation effect in dense fluids, previously seen for guest molecules diffusing within porous solids. The voids in the larger component have been characterized in terms of void and neck distributions by means of Voronoi polyhedral analysis. Four different mixtures with differing ratios of guest to host diffusivities (D) have been studied. The results suggest that the diffusion anomaly is seen in both close-packed solids with disorder and dense fluids. In the latter, the void network is constantly and dynamically changing and possesses a considerable degree of disorder. The two regimes, viz., the linear regime (LR) and the anomalous regime (AR), found for porous solids are shown to exist for a dense medium as well. The linear regime is characterized by $D_g \propto 1/\sigma_{gg}^2$, where σ_{gg} is the diameter of the guest. The anomalous regime exhibits a maximum in D up to rather high temperatures ($T^* = 1.663$), even though in porous solids the maximum disappears at higher temperatures. In agreement with previous studies on porous solids, a particle in the AR is associated with lower activation energy, lower friction, and less backscattering in the velocity autocorrelation function when compared to a particle in the LR. Wavevector dependent self-diffusivity, Δ, and decay of the intermediate scattering function, $F_s(k, t)$, exhibit contrasting behaviors for the LR and AR. For LR, Δ exhibits a minimum at values of k at which there are spatial correlations in $S(k)$ while a smooth decrease with k is seen for AR. For LR, $F_s(k, t)$ shows a biexponential decay corresponding to two different time scales of motion. Probably, the fast decay is associated with motion within the first shell of solvent neighbors and the slow decay with motion past these shells. For AR, a single-exponential decay is seen. The results indicate a breakdown of the Stokes−Einstein (SE) relationship. The relevant quantity that determines the validity of the SE relationship is the levitation parameter which is indirectly related to the solute/solvent radius ratio and not either the size of the solute or the solvent alone.

1. Introduction

In the past decade, studies on fluids confined within porous solids have yielded some surprising results. Several of these pertain to the transport properties of confined fluids. For example, sorbates confined within single walled nanotubes[1−4] show superdiffusive motion where mean squared displacement $u^2(t) \approx t^\alpha$, $\alpha > 1$. In contrast, sorbates in zeolites have always exhibited diffusive[1−4] behavior, $u^2(t) \approx t$. Single-file diffusion of sorbates confined within one-dimensional cylindrical pores exhibits a $\sqrt{t}$ dependence of the mean square displacement.[5,6] Earlier, pulsed field gradient NMR measurements of sorbates within zeolites showed the existence of at least five different types of dependences of self-diffusivity, D, on concentration, c, of sorbates.[7] Many of these D vs c behaviors are unexpected and have interesting explanations.[8]

Another interesting observation is the maximum in self-diffusivity, D, for fluids confined in porous solids as a function of their size. The maximum is found when the size of the diffusant is comparable to the diameter of the void.[9] Two distinct dependences of self-diffusivity on size have been observed. The linear regime (LR), where $D \propto 1/\sigma_{gg}^2$, is observed for sizes of guest (σ_{gg}) which are significantly smaller than the void diameter (σ_w). The anomalous regime (AR), characterized by a maximum in D, has been observed for particle diameter approaching that of the void diameter of the porous solid (Figure 1a). There is a regime within AR where *the self-diffusivity increases with the size of the diffusant*. This anomalous maximum in D is counterintuitive and is known as the *levitation effect* (LE), for the following reasons: When a guest particle has a diameter derived from the LR of the LE, its diameter is small relative to the window diameter. When such a guest passes through the bottleneck for diffusion, namely, the window, it is essentially interacting favorably or strongly with only a few of the host atoms. This can be seen from Figure 1b where most of the atoms of the host are at a relatively large distance where the interaction is weak. Zeolite Y and A consist of large α-cages with a diameter of 11.8 Å interconnected via narrower windows with diameters of 7.5 and 4.0 Å, respectively. When the guest atom is inside the α-cage, the guest atom is in the proximity of a larger number of host atoms, comprising the two-dimensional surface of the α-cage. Thus, it interacts favorably with a larger number of host atoms inside the cage. The magnitude of interaction energy at the window is, therefore, significantly lower than that seen when the guest is located within the α-cage. This

[†] Solid State and Structural Chemistry Unit.
[‡] Center for Condensed Matter Theory.
[§] Also at the Jawaharlal Nehru Centre for Advanced Scientific Research, Jakkur, Bangalore, India.

10.1021/jp046312w CCC: $30.25
Published on Web 03/03/2005

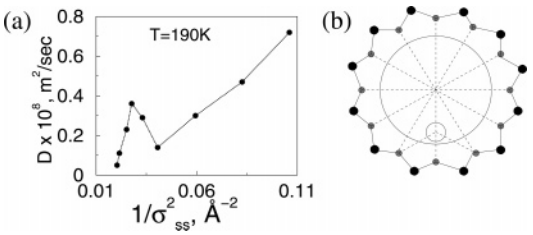

Figure 1. (a) Plot of self-diffusivity vs $1/\sigma_{gg}^2$ in NaY. (b) The bottleneck for diffusion is the 12-membered ring or window in zeolite NaY.[9] This is shown by the black circles or dots: Si, larger circles; O, smaller circles; line, the Si−O bond. The guest atoms are shown by unfilled circles. For the larger guest with diameter comparable to that of the 12-ring window, there is net cancellation of forces; this does not happen for the smaller guest.

results in a relatively large difference in energy, and the energy barrier for the smaller particle is, therefore, large and positive.

For a guest particle whose size is comparable to the window diameter (from AR), the interaction with the host atoms of the window is highly favorable as it interacts optimally with almost all of the atoms at the window. As a result, the interaction energy, at the window, is comparable in magnitude or sometimes larger in magnitude than that within the α-cage. As a consequence, the energy barrier at the window is small, zero, or even negative. Thus, a sorbate or guest whose size is comparable to the window and from AR has a lower activation energy for diffusion than that of a guest whose size is smaller relative to the window (and from LR), the bottleneck for diffusion.

While this provides an explanation for the observed maximum in *D*, this explanation makes use of the pore structure of zeolites Y and A. It is, therefore, specific to zeolites Y and A and to those zeolites with structures consisting of cages interconnected via narrow windows. Studies in other zeolites with completely different pore structures, such as purely cylindrical channels as in $AlPO_4$-5 or straight and sinusoidal channels running along perpendicular directions as in silicalite, also exhibit similar diffusion maxima. Thus, a more general explanation which can account for LE regardless of the pore structure is required. This explanation of LE is provided in terms of the force acting on the guest by the confining medium, namely, zeolites. Both explanations are related to each other. The diffusion maximum owes its origin to the symmetry around the diffusant at one or more points along the diffusion path within the confining medium. Such symmetry leads to mutual cancellation of forces exerted on the guest by the confining medium (e.g., zeolite, the host), for a particle that is in the anomalous regime.[9] For example, in zeolite Y (Figure 1b), a spherical sorbate of diameter 6.0 Å has dimensions comparable to[9] those of the bottleneck for diffusion, the 12-ring window made up of Si and O atoms, and the force exerted on the guest by the host located at one side is, by symmetry, exactly equal and opposite to that exerted by the host located diagonally opposite. Thus, the forces essentially cancel each other when the guest is located at the window. The mutual cancellation of forces results in negligible net force on the guest even though the magnitude of the guest−host interaction energy is large. Such cancellation does not occur in the case of the smaller guest from the linear regime (smaller open circle) as it is not equidistant from all atoms of the 12-ring window. Although, here, we have used the structure of zeolite Y as an example, such a situation can arise in any zeolite. For example, in silicalite or VPI-5 a similar situation exists. In fact, in cylindrical channels of uniform diameter such cancellation occurs throughout the channel. In comparison, such cancellation in zeolite Y or A occurs only near the window.

The force exerted on the guest by the host, in principle, could be either dispersion forces, which are attractive in nature, or repulsive forces at short distances. Although, at first glance, it appears that the diffusion maximum has its origin in the repulsive forces, it is not so. The forces are predominantly attractive and arise from dispersion interactions which, in the case of the Lennard-Jones potential, are due to the $-1/r^6$ term. We have previously demonstrated this, in an unambiguous manner,[9] by carrying out MD simulations in which the interactions between the guest and the host were modeled in terms of purely repulsive interactions using only the $1/r^{12}$ term. In these simulations, no diffusion maximum was seen. This clearly shows the role of attractive dispersion interactions in giving rise to the diffusion maximum or LE.

Note that the reduced force on the guest (from AR) at the window in zeolite Y is essentially that of the component of the force that is perpendicular to the direction of motion $\mathbf{F}_\perp$. How is the motion altered by the decrease in $\mathbf{F}_\perp$? A reduction in $\mathbf{F}_\perp$ essentially decreases the attraction of the guest to the zeolite surface. Consequently, the guest particle is less strongly bound. Any particle that is bound less strongly is freer to diffuse. To clarify, consider a situation where the host medium is exerting a force, $\mathbf{F}$, on the guest particle. The force has a component, $\mathbf{F}_{||}$, in the direction of motion and component, $\mathbf{F}_\perp$, in the direction perpendicular to the direction of motion, so that $\mathbf{F} = \mathbf{F}_{||} + \mathbf{F}_\perp$. If the magnitude of $\mathbf{F}_\perp \gg \mathbf{F}_{||}$, then it is clear that the guest will not diffuse since it is being strongly attracted by the zeolite surface, and in the limit when $\mathbf{F}_\perp$ approaches zero, the diffusivity is at a maximum. Thus, changes in $\mathbf{F}_\perp$ also affect or alter *D*.

To be precise, the diffusion maximum is seen when the dimensionless levitation parameter defined by

$$\gamma = \frac{\sigma_{opt}}{\sigma_{neck}} = \frac{2 \times 2^{1/6}\sigma_{gh}}{\sigma_w} \qquad (1)$$

approaches unity for a guest in crystalline solids. In other words, the anomalous maximum is seen when γ approaches unity. Here, σ_{opt} is the optimum distance at which interactions between the sorbate and the host medium are most favorable, and σ_{neck} is the diameter of the neck interconnecting two voids. For simple systems interacting with the (6−12) Lennard-Jones (LJ) potential, this can be expressed as the second expression on the right, where σ_{gh} is the guest−host Lennard-Jones interaction parameter, and σ_w is the window diameter. The levitation effect has been found in all types of porous solids, such as zeolites, aluminophosphates, etc., regardless of the geometrical and topological details as well as the chemical nature of pore network.[10] For systems with purely repulsive interactions and no attractive dispersion interactions, no diffusivity maximum is found.[9] Further, in systems with a considerable degree of disorder and a wide distribution of pore dimensions, it is difficult to define a unique value for σ_w, and it has been observed that the maximum in the levitation effect occurs at values of γ considerably lower than unity.[11]

Most liquids, such as liquid argon, water, ethanol, etc., fall in the class of dense fluids and do not possess voids of the sizes seen in porous solids. However, it is well-known that even amidst such dense fluids or solids there are voids. In the closest packing of *N* spheres of radius *R*, there are 2*N* tetrahedral (diameter $\approx 0.450R$) and *N* octahedral voids (diameter $\approx 0.828R$). The neck dimension (the narrowest void dimension between two octahedral or tetrahedral voids) is still smaller.

The neck between two tetrahedral voids and two octahedral voids has the same dimension and equals $0.155R$.[12] A relatively smaller particle can, therefore, easily diffuse through a solid made up of larger particles. Thus, a reasonably large solute can exist in the voids amidst the closest packing of spheres (namely, a solid) of a somewhat larger size. It is, therefore, reasonable to assume that voids of similar or larger dimensions exist in liquids.

Self-diffusivity of a solute in a fluid or a solvent has been extensively investigated. It is related to friction through the well-known Stokes−Einstein relation.[13]

$$D = \frac{kT}{\zeta_{\text{total}}} \tag{2}$$

Here, $\zeta_{\text{total}} = 6\pi a\eta$ where k is the Boltzmann constant, η is the solvent viscosity, and a is the solute radius. Frequently, in these studies, the focus is on the mobility of an ion in a polar solvent, as conductivity of an ion is easily measured in comparison to diffusivity. In such polar systems, the total friction, ζ_{total}, is the sum of the terms from the bare ion and the friction due to the electrostatic and induction interactions between the ions and the solvent molecules, termed the dielectric friction, ζ_{DF}.

$$\zeta_{\text{total}} = \zeta_{\text{bare}} + \zeta_{\text{DF}} \tag{3}$$

For the ions in polar solvents, the dielectric friction is often the predominant term. In comparison to ζ_{DF}, ζ_{bare} is small.[14] In systems with negligible electrostatic interaction or induction interaction, ζ_{bare} is the predominant term. There are a number of studies which investigate how ζ_{DF} varies for a number of ions in a variety of polar solvents.[15,16] Recently, several groups have attempted to explain the observed maximum of ionic conductivity in terms of the changes in hydrogen bonding.[17−20] We are not aware of any detailed investigation into variation of ζ_{bare} with size. The Stokes−Einstein relation has been observed to be valid for a wide range of solute radius a. For example, it has been found to be valid for polymers dissolved in solvents. However, when the solute radius is small the Stokes−Einstein relationship is often not obeyed.[13,21]

Here, we investigate the variation of self-diffusivity and friction of an uncharged solute in a solvent. We consider a binary mixture consisting of two components. One of the components has a larger radius, while the other component, with a smaller radius, is varied. Given the ubiquity of the levitation effect in porous solids, depending only on gross structural features, it is of interest to ask if the levitation effect is also present in dense materials and, in particular, dense liquids and solids. This question is of great relevance for a fundamental understanding of diffusion and friction as well as ionic conductivity in solvents. Many chemical reactions and biochemical processes occur in solvents, and their rate is often determined by how fast the products and reactants can diffuse within those solvents.[22,23] We address this question by performing classical molecular dynamics simulations on a binary mixture composed of particles interacting via the Lennard-Jones potential. In mixtures of several components, the smaller component might be able to find a percolating path through the medium consisting of the larger component. Consequently, the smaller component might actually diffuse through the medium. We examine the size dependence of the diffusion coefficient of the smaller component through a medium consisting of the larger component.

2. Methodology

2.1. Intermolecular Potential Functions. The guest−guest, guest−host, and host−host interactions have been modeled in terms of short range (6−12) Lennard−Jones potential

$$\phi_{\alpha\beta}(r_{\alpha\beta}) = 4\epsilon_{\alpha\beta}[(\sigma_{\alpha\beta}/r_{\alpha\beta})^{12} - (\sigma_{\alpha\beta}/r_{\alpha\beta})^{6}] \tag{4}$$

where $r_{\alpha\beta}$ is the interparticle separation, and α, $\beta = 1, 2$ refer to the particle type (host or guest). The total potential energy of the system is

$$\Phi(r) = \sum_{i=1}^{N_h}\sum_{j=1}^{N_g}\phi_{gh}(r) + \sum_{i=1}^{N_g}\sum_{j>i}^{N_g}\phi_{gg}(r) + \sum_{i=1}^{N_h}\sum_{j>i}^{N_h}\phi_{hh}(r) \tag{5}$$

where N_h is the number of hosts and N_g is the number of guests present in the system. We use the non-Lorentz−Berthelot rule for the cross interaction parameters. There are many systems that do not obey the Lorentz−Berthelot combination rule (see, for example, AgI[24,25]).

2.2. Molecular Dynamics Simulations. All calculations have been carried out in the microcanonical ensemble (NVE). Cubic boundary conditions have been employed. Molecular dynamics (MD) integration was carried out with the use of the velocity Verlet algorithm.[26] All of the atoms (guest and host) are included in the MD integration.

2.3. Voronoi Polyhedra Analysis. To characterize the structure of the "pore space" or "void space" in the host matrix, we used the Voronoi construction which has been employed in similar studies of liquids[27,28] and other disordered materials, such as porous media and powders,[29,30] resulting in valuable insights into the distribution of voids within these systems. In any specified configuration of equal-sized particles, the Voronoi polyhedron of a given particle, i, is the set (subvolume) of all points that are closer to i than to any other. The vertexes and edges of the Voronoi polyhedra are, by construction, equally far from the closest surrounding particles. Specifically, in disordered configurations, a Voronoi vertex is equidistant from 4 particles, and any point on a Voronoi edge is equidistant from 3 particles. Therefore, a natural and convenient description of the empty or void space can be given in terms of the network formed by the edges of the Voronoi polyhedra. Specifically, one can visualize the void space as made of "pores" each of a radius given by the distance of a Voronoi vertex to the surrounding particles *minus* the particle radius. These pores are interconnected through "channels" whose radius is given by the smallest lateral distance of a Voronoi edge and the surrounding particles *minus* the particle radius. We refer to the corresponding diameters as *void* and *neck* sizes, respectively. Figure 2 illustrates these for two dimensions. Diffusants of a given radius can find an interconnected path between voids if the intervening neck (or channel) sizes are larger than the diffusant radius. However, the motion of the host atoms ensures that the void network is restructured dynamically. Thus, even a guest particle for which there is no interconnected path at a given time step manages to diffuse over a period of time.

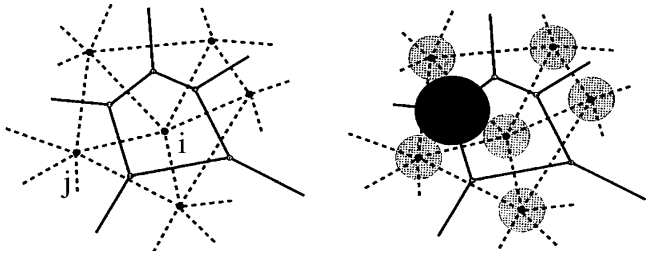

Figure 2. Two-dimensional illustration of the Voronoi−Delaunay dual construction. The central atom, *i*, is surrounded by atoms, *j*. This figure was taken from ref 27.

TABLE 1: Details of the Four Sets of Molecular Dynamics Calculation on Guest−Host (Solute−Solvent) Systems[a]

set	ϵ_{hh} (kJ/mol)	m_h (amu)
I	1.84	85
II	0.99	85
III	0.25	85
IV	0.25	40

[a] $\sigma_{hh} = 4.1$ Å, $m_g = 40$ amu, $\epsilon_{gg} = 0.99$ kJ/mol, and $\epsilon_{gh} = 1.50$ kJ/mol.

Voronoi and Delaunay tessellations have been carried out using the algorithm by Tanemura et al.,[31] as outlined in Sastry et al.[28] The main purpose of the Voronoi analysis is to obtain the distribution of void and neck diameters. For diffusion within crystalline porous solids, the anomalous maximum in the self-diffusivity occurs when γ is close to unity. For diffusion within disordered systems,[32] the maximum occurs at values of γ significantly less than unity when one uses the mean neck size to obtain σ_{neck}. The variability of the neck size clearly matters, and the narrowest neck size along a given path determines if guest particle diffusion along that path is possible.

2.4. Computational Details. The number of atoms of the solvent or host, N_h, and solute or guest, N_g, are 500 and 50, respectively. Molecular dynamics simulations have been carried out at 50 K, which corresponds to different reduced temperatures for the four sets. $T^* = k_B T/\epsilon_{hh} = 0.226$, 0.420, 1.663, and 1.663 for sets I, II, III, and IV, respectively. A time step of 5.0 fs is adequate to obtain good energy conservation (1 in 10^4). The duration of the equilibration is 1.0 ns, and averages are accumulated over another 1.0 ns. The positions and velocities were stored every 0.25 ps for the calculation of properties. Calculation of the void and neck distributions has been carried out using 400 of these configurations. Other properties were averaged over all of the stored configurations. Simulations were performed in a cubic cell 33.3 Å in length with a cutoff radius of 16.5 Å.

Interactions between the guest and the host atoms were computed using the rule $\sigma_{gh} = \sigma_{gg} + 0.7$ Å. Many liquid mixtures deviate from the Lorentz−Berthelot rule.[33] This is generally true when the solute interacts strongly with the solvent. The density we have chosen ($\rho^* = 0.933$) for the four sets is higher than that of the triple point density which is typically around 0.7. All properties indicated by asterisks are in reduced units.

Four different sets of calculations were carried out. Table 1 lists the relevant details of the four sets. In these sets, we attempted to vary the mobility of the host or the solvent (larger) particles. To achieve this, we have changed the value of ϵ_{hh} or the mass, m_h. For set I, $\epsilon_{hh} = 1.84$ kJ/mol. It is 0.99 kJ/mol for set II and 0.25 kJ/mol for sets III and IV. For each run, the void and neck sizes are calculated for 400 configurations using the positions of the host particles.

3. Results and Discussions

3.1. Host (or Solvent) Structure. The host radial distribution functions (rdfs) for all sets are shown in Figure 3. Although, the runs were made at 50 K for all four sets, this corresponds to different reduced temperatures for the four sets. $T^* = 0.226$, 0.420, 1.663, and 1.663 for sets I, II, III, and IV, respectively. The host is essentially a frozen solid in set I which is what one expects at $T^* = 0.226$. But from the position and intensity of the peaks in the rdf, it evident that the host is a face-centered (fcc) solid with some defects. This is also evident from the snapshot (see Figure 4) which clearly shows the existence of well-defined planes which will yield the diffraction patterns of

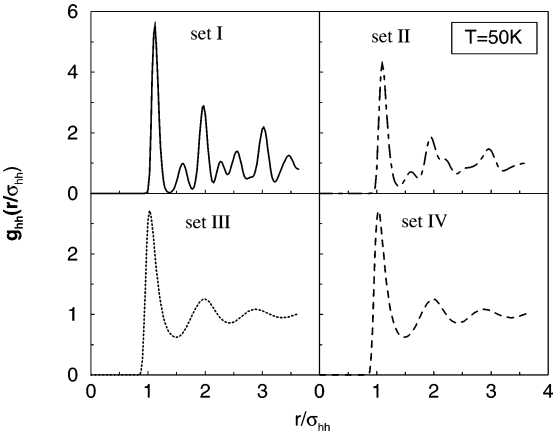

Figure 3. Host or solvent rdfs for the four sets of parameters.

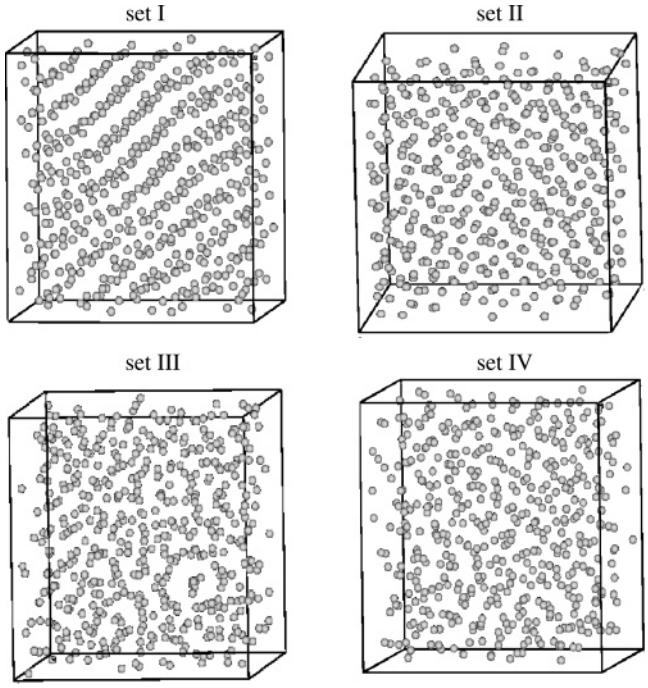

Figure 4. Snapshot of the host structure for the four different sets.

an fcc solid. The rdf for set II suggests that the host is frozen ($T^* = 0.420$) but the structure now has a larger degree of disorder. This is also evident from Figures 3 and 4. The second peak in the rdf of set II appears to be split and suggests that it may be an amorphous solid. As we shall see, the void and neck distributions are also suggestive of an amorphous solid. The rdfs for sets III and IV correspond to a liquid state. Thus, the four sets represent a range extending from close-packed solids with few defects (set I) to amorphous solids and to liquids (set IV). Figure 4 shows a snapshot of the host structure for the four sets.

The void distribution, $g_v(d^*)$, of the void diameters, d^*, for this liquid phase has been computed from Voronoi analysis and is shown in Figure 5a. Neck distribution $g_n(d^*)$ is shown in Figure 5b. The neck distribution peaks at a lower value of $d^* = d/\sigma_{hh}$, where d^* is the diameter of the void or neck. A bimodal distribution of voids is seen in Figure 5a for set I. The void-size distribution of the disordered fcc crystal exhibits two peaks at void sizes of $d^* = 0.35$ and 0.55. This is in agreement with the previously calculated void distribution for a fcc solid by Corti et al.[27] The peaks at $d^* = 0.35$ and 0.55 correspond to the tetrahedral and octahedral voids, respectively,[24] in the fcc

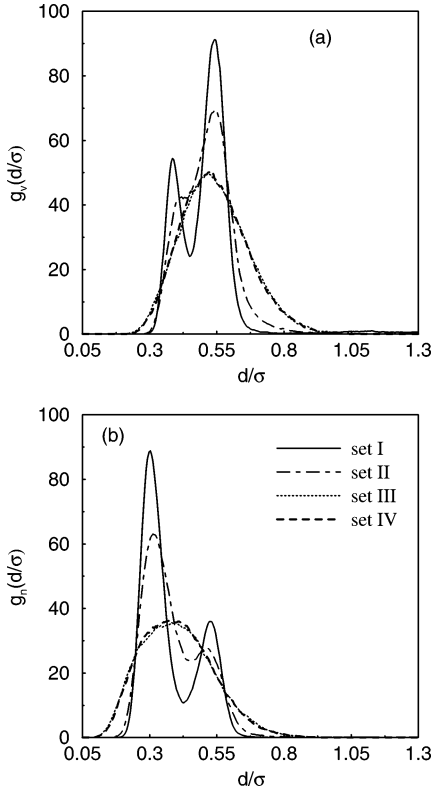

Figure 5. Distribution of (a) void and (b) neck diameters, d/σ_{hh}, of the host for four different sets of runs. The ordinate was obtained by binning the void and neck radius with a bin size of $\Delta r_n = 0.01$ Å and finally dividing by the total number of configurations used.

crystal. Although the first and second peaks of the distribution are not aligned exactly with the fcc crystal's void-size distribution, it is clear that the inherent structures of the bimodal distribution are related to the void in the fcc crystal. In fact, the bimodal distribution is caused by the formation of distorted tetrahedra and octahedra. Note that the characteristic double peak in the void-size distribution was also seen by Finney and Wallace in a study of random packing of soft spheres.[35] For set II, no distinct bimodal distribution is seen. This suggests that tetrahedral and octahedral voids cannot be clearly identified suggesting that the structure is disordered. For liquid phases, as expected,[27] the distribution is unimodal. Most of these arguments are applicable to the neck distribution, $g_n(d^*)$, as well, and they exhibit behaviors similar to that of $g_v(d^*)$, although the distribution maximum occurs at a lower value of d^*.

3.2. Dynamical Properties. *3.2.1. Dependence of Tracer or Self-Diffusivity on Solute/Guest Size.* Figures 6 and 7 show the mean square displacement (msd) of guests (a and b) and hosts (c and d) for the four different sets at 50 K. Self-diffusivities of the guest particles have been computed using Einstein's relationship[26]

$$D = \langle u^2(t)\rangle/2d_i t \tag{6}$$

with d_i taken as 3 and the mean square displacement, $u^2(t)$, computed from the MD trajectories averaged over all initial times and guest particles. The self-diffusivity values are listed in Table 2, and they are plotted in Figure 8 against the reciprocal of the square of the sorbate diameter, $1/\sigma_{gg}^2$. For small values of σ_{gg}, the relationship $D \propto 1/\sigma_{gg}^2$ which is expected on the basis of kinetic theory is shown to be valid. For large values of σ_{gg}, *a maximum* is seen for a particular size of guest.

Previous simulations of diffusants confined to *porous solids* suggest that the self-diffusivity exhibits a maximum when its size is comparable to the void dimension through which it is diffusing.[9] The results here confirm that *the existence of an anomalous maximum in self-diffusivity*, termed the *levitation effect*, is seen in *dense* liquids as well.

Relative Mobilities of Guest−Host and Levitation Effect. The host is mobile, and the diffusivities of the host are 0.28×10^{-11}, 0.80×10^{-11}, 0.12×10^{-8}, and 0.20×10^{-8} m^2/s for sets I, II, III, and IV, respectively. This may be compared to a guest diffusivity on the order of 0.85×10^{-8} m^2/s. The ratio of self-diffusivities of the guest to the host (D_g/D_h) is 3035, 1062, 7, and 4 for sets I, II, III, and IV, respectively. The host for set I is nearly frozen when compared to the guest. The host for set IV is nearly as mobile as the guest. Thus, the four sets span a wide range of guest−host dynamics going from one extreme to another. It is worth noting that the diffusion maximum is seen in all of these widely differing dynamics of host vis-à-vis guest. The maximum relative to the minimum in self-diffusivity (seen at the junction between the linear and anomalous regimes) for sets III and IV suggests that the maximum is not that intense. In contrast, the height of the diffusivity maximum is significant for sets I and II. The temperature of the system for sets III and IV is significantly high ($T^* = 1.663$). The high temperature implies a considerable degree of disorder and a relatively high mobility associated with the host. The void network is frequently and dynamically altered. It is surprising that, despite this, the diffusion maximum persists. This may be contrasted with zeolites where the diffusion maximum is seen to disappear at high temperatures.[36] It appears that in dense liquids the diffusion maximum persists up to a relatively higher temperature. This may be attributed to the larger number of host neighbors and the stronger or more favorable interaction with those neighbors.

To determine if the increase in self-diffusivity of the guest, at a particular size, is associated with a similiar increase in the self-diffusivity of the host, we plotted the ratio D_g/D_h as a function of the size of the guest σ_{gg} for the four sets (Figure 10). The diffusivity maximum of the guest is relative to the host suggesting that the guest is diffusing at a faster rate than the host. Note that for set I the ratio is quite large and that for sets III and IV it is not large. Clearly, a size dependent maximum of the guest exists relative to the host and for a range of host diffusion coefficients.

In Figure 11, we show the variation of the ratio of the guest to the host as a function of temperature for two sizes, one from LR and another from AR. Note that at low temperatures, the particle from AR has a higher ratio than the particle from LR but at higher temperatures, the reverse is true. Earlier, Yashonath and Chitra[36] reported the self-diffusivity of the guest from LR and AR in zeolite Y as a function of reciprocal temperature and noted the existence of a temperature above which the order of D is reversed. Thus, any experimental verification of these results using just two guests of differing sizes needs to be performed at a temperature lower than this crossover temperature to observe that the larger guest has a higher diffusivity than the smaller guest.

3.2.2. Disorder in Host or Solvent Structure and Levitation Parameter. For diffusion within crystalline porous solids, the anomalous maximum in the self-diffusivity occurs when γ is close to unity. Figure 9 shows a plot of D against γ for the four sets. Note that with an increase in disorder, there is a shift in the maximum toward a lower γ. For example, for sets III and IV the maximum is $\gamma \approx 0.62$, and for sets I and II, it is $\gamma \approx 0.74$. For diffusion within disordered systems,[32] the maximum

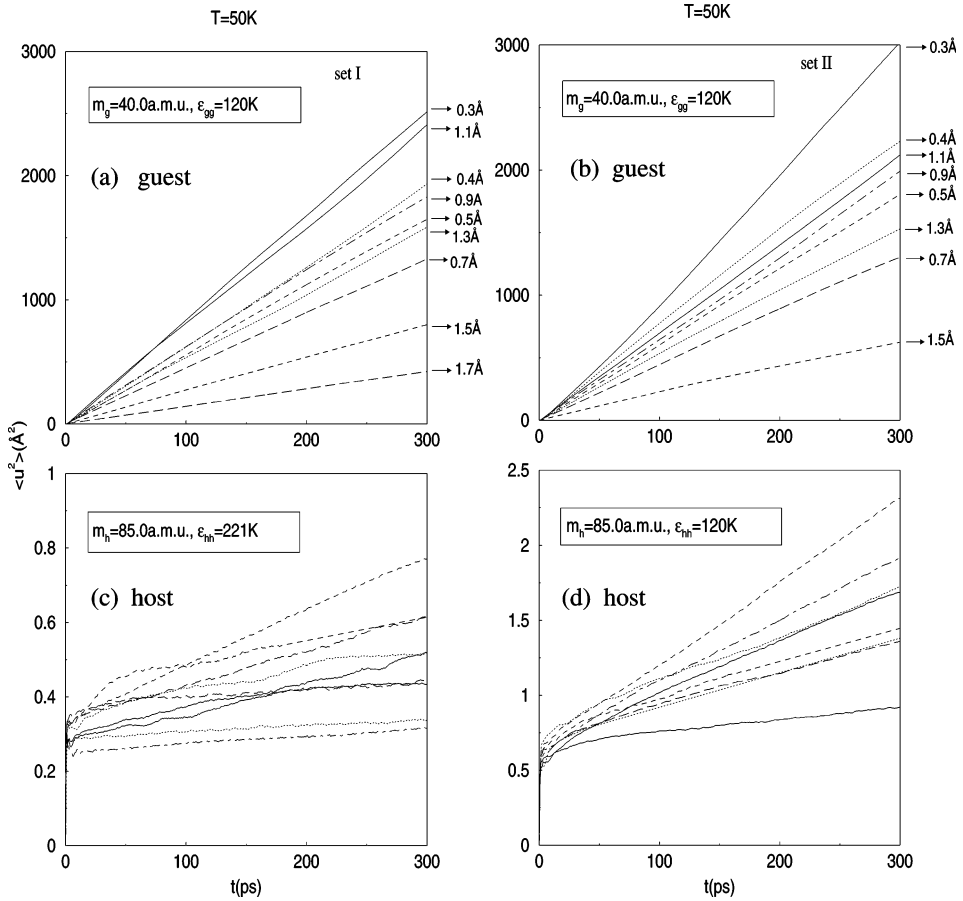

Figure 6. Mean square displacement, $u^2(t)$, of sets I and II at 50 K. For guest (a and b) and host (c and d). Guest sizes are indicated on the right.

occurs at values of γ significantly less than unity. This probably happens because of the absence of a unique neck diameter. Instead, the neck diameter has a wide distribution making it difficult to define σ_w. This makes it difficult to define γ precisely. Further, the smallest neck sizes in the distribution probably provide the bottleneck for diffusion and, therefore, influence diffusion more strongly. Also, at finite temperatures, the thermal motion of the host decreases the probability of passage of the guest particles through the necks.

3.2.3. Lowered Force on the Guest and Activation Energies of LR and AR. There are a number of factors, such as mass, interaction energy, size, etc., that influence the self-diffusivity of a diffusant. However, the observed maximum in self-diffusivity from the levitation effect has several special characteristics, two of which follow: (i) the average force on the guest exerted by the medium in which the guest is diffusing is a minimum for the particle for which self-diffusivity is a maximum (particles whose sizes lie in the linear regime experience a larger force)[9] and (ii) a particle in the anomalous regime is also associated with a lower activation energy when compared to those in the linear regime.[36,37] To confirm that the underlying cause for the observed maximum in *D*, in the present case, is the levitation effect, the force on the guest arising from the presence of the host, $\vec{F}_{gh}$, has been computed. $\vec{F}_{gh}$ is plotted in Figure 12 for different sizes of sorbates or guests. The force is minimum for a particular value of σ_{gg} which corresponds to the maximum in *D* (see Figure 12). The maximum is due to the mutual cancellation of the forces exerted on the diffusant by the host medium (in which the diffusant is moving) as already explained (Figure 1). This mutual cancellation occurs for a particular size of guest. *The size of the guest at which such mutual cancellation occurs depends on the neck diameter through which it is diffusing.*

The activation energy of the diffusants in the linear regime has previously been found to be higher than that of those in the anomalous regime. We have computed this for set III. Table 3 lists the values of self-diffusivity at four different temperatures for $\sigma_{gg} = 0.7$ Å and $\sigma_{gg} = 0.9$ Å. Figure 13 shows the Arrhenius plot of the self-diffusivity, *D*. Activation energies have been calculated from the slope of the straight line obtained from a least-squares fit to the data. The value of the activation energy for the 0.7 Å particle is 1.21 kJ/mol. For a 0.9 Å particle, $E_a =$ 0.77 kJ/mol. This clearly shows that the activation energy is lower for the particle in the anomalous regime. These results are consistent with the behavior of guests in porous solids such as zeolite NaY, NaCaA, etc., reported previously.[36]

3.2.4. Friction and van Hove Correlation Function. We have computed the friction, ζ_{bare}, on the guest particles from the force−force autocorrelation function

$$\zeta_{bare} = \frac{1}{3k_BT}\int_0^\infty \langle \mathbf{F}_i(t)\cdot\mathbf{F}_i(0)\rangle \mathrm{d}t \qquad (7)$$

where $F_i(t)$ is the random force on a solute at time *t* and $\langle \mathbf{F}_i(t)\cdot\mathbf{F}_i(0)\rangle$ is the equilibrium random force autocorrelation function on this solute.

They are listed in Table 4. The values for friction obtained for the smaller guest in the linear regime are always higher than the friction experienced by the larger guest in the anomalous regime.

Figure 14 shows the velocity autocorrelation function (vacf) for the particle in the linear and anomalous regimes correspond-

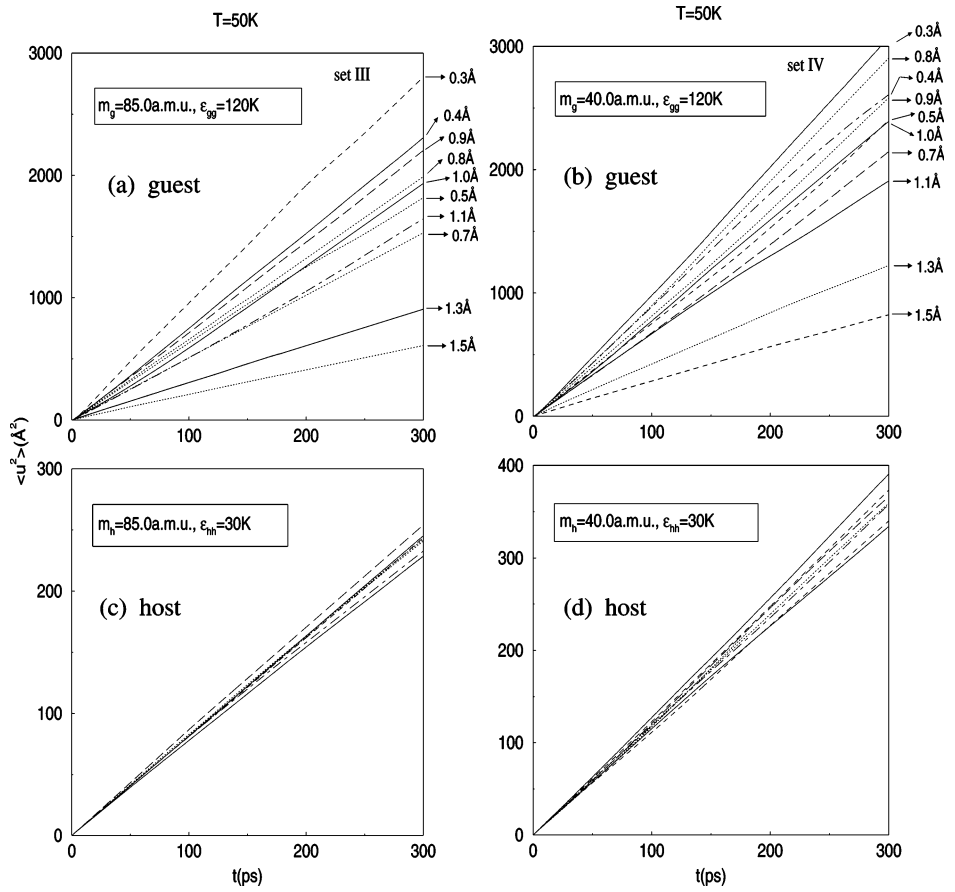

Figure 7. Mean square displacement, $u^2(t)$, of sets III and IV at 50 K. For guest (a and b) and host (c and d). Guest sizes are indicated on the right.

TABLE 2: Self-Diffusivity Values for All Sets at 50 K

	D ($\times 10^8$ m^2/s)			
σ_{gg} (Å)	set I[a]	set II[b]	set III[c]	set IV[d]
0.3	1.41	1.70	1.72	1.73
0.4	1.07	1.20	1.26	1.44
0.5	0.93	0.98	1.01	1.32
0.7	0.74	0.73	0.85	1.21
0.8	−	−	1.11	1.43
0.9	1.02	1.10	1.23	1.49
1.0	−	−	1.02	1.34
1.1	1.31	1.17	0.92	1.06
1.3	0.87	0.88	0.56	0.68
1.5	0.45	0.37	0.20	0.46

[a] $D_{host} = 0.28 \times 10^{-11}$ m^2/s. [b] $D_{host} = 0.80 \times 10^{-11}$ m^2/s. [c] $D_{host} = 0.12 \times 10^{-8}$ m^2/s. [d] $D_{host} = 0.20 \times 10^{-8}$ m^2/s.

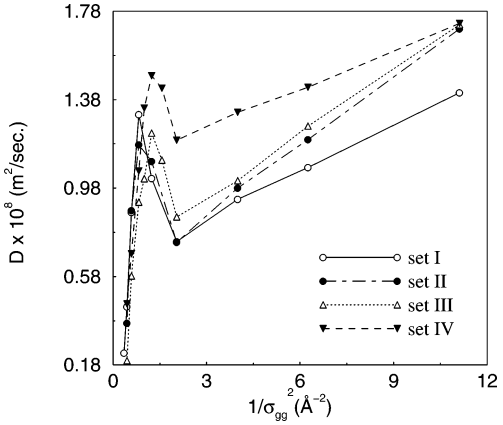

Figure 8. Self-diffusivity of the guest, D, against reciprocal of the square of the sorbate diameter.

ing to four different host structures or sets. For all cases, the smaller particle in the linear regime (here, we have chosen $\sigma_{gg} = 0.7$ Å) exhibits a significant negative correlation which is absent for the larger particle in the anomalous regime (for example, $\sigma_{gg} = 0.9$ Å). Previous studies on monatomic sorbates[9,38] and linear molecules[39] have shown that the potential energy surface is relatively flat for a particle in the anomalous regime. The vacf obtained here confirms that the potential energy surface is flat for the anomalous regime even among the densely disordered liquids and solids.

3.2.5. Wavevector Dependence of the Width of the Dynamic Structure Factor. We now investigate the dependence of the diffusion properties on wavenumber, k, for intermediate k values. In the hydrodynamic limit ($k \rightarrow 0$, $\omega \rightarrow 0$), the simple diffusion model is valid, and the full width at half-maximum (fwhm), $\Delta\omega$, of the dynamic structure factor, $S_s(k, \omega)$, is proportional to $2Dk^2$. The motion in the intermediate range of k values is strongly influenced by the intermolecular potential. Previous simulation studies[9] of guests of varying sizes in zeolites suggest that intermolecular interactions play an important role in the levitation effect. For example, for systems interacting with a purely repulsive term (with no attractive dispersion term), the diffusivity maximum or levitation effect is not seen.[9] We, therefore, may be able to find some signature of the LE if we look at the variation of the self-diffusivity at an intermediate k regime. We have computed the $\Delta\omega(k)$ in the intermediate k-region for a particle from the linear and the anomalous regimes. Note that the full width at half-maximum of the self-part of $S_s(k, \omega)$ provides an estimate of the magnitude of the self-diffusivity, $\Delta\omega(k) \propto D(k)$. The dynamic structure factor, $S_s(k, \omega)$, was obtained from the Fourier transform of the

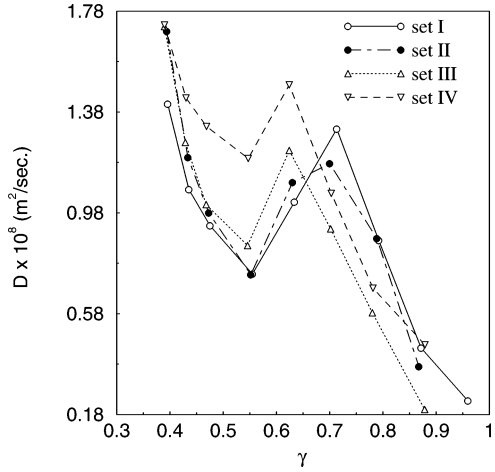

Figure 9. Self-diffusivity of the guest, D, against γ for all the sets.

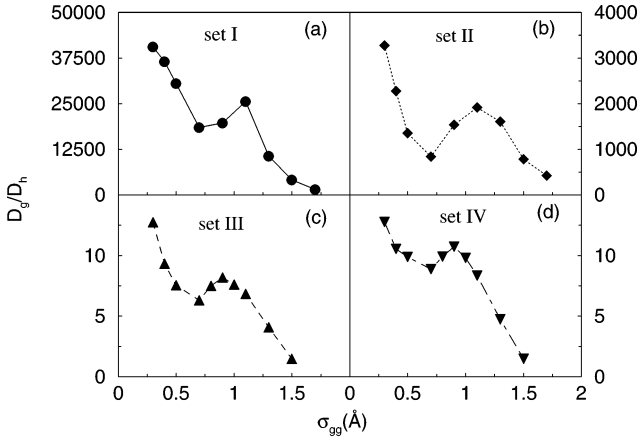

Figure 10. Variation of the ratio of the guest to host self-diffusivity, D_g/D_h, with guest diameter, σ_{gg}, for the four sets.

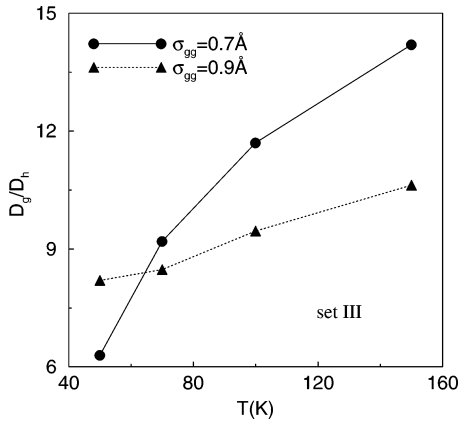

Figure 11. Variation of the ratio of the guest to host self-diffusivity, D_g/D_h, as a function of temperature for set III.

intermediate scattering function, $F_s(k, t)$, for several sizes of the guest. $F_s(k, t)$ was computed by taking a powder average.[40]

Previously, Nijboer and Rahman[41] and Levesque and Verlet[42] investigated the variation of the ratio $\eta(k) = \Delta\omega/2Dk^2$ with k for argon. They investigated the variation of $\eta(k)$ for two thermodynamic states, $\rho^* = 0.8442$, $T^* = 0.722$, a high-density fluid and $\rho^* = 0.65$, $T^* = 1.872$, a low-density fluid. Nijboer and Rahman[41] found that the variation of $\Delta\omega(k)/2Dk^2$ for high-density fluid at low temperature ($\rho^* = 0.8442$, $T^* = 0.722$) exhibits a minimum and a maximum. The minimum in $\Delta\omega(k)$ was found to correspond to the k value at which strong

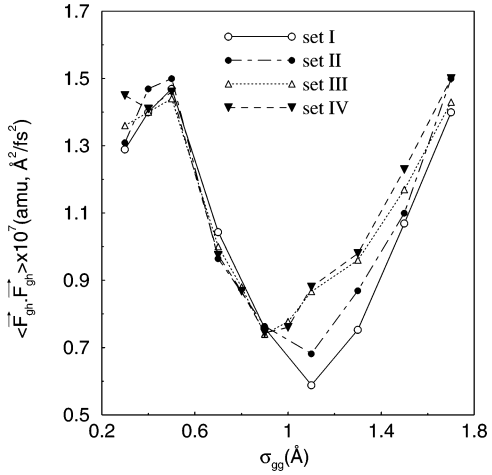

Figure 12. $\vec{F}_{gh}$ for different sizes of the guest for the four sets.

TABLE 3: Self-Diffusivity Values at Different Temperatures for Set III for Two Different Sized Particles, One from the Linear Regime ($\sigma_{gg} = 0.7$ Å) and Another from the Anomalous Regime ($\sigma_{gg} = 0.9$ Å)

temperature (K)	D^a ($\times 10^8$ m^2/s)	D^b ($\times 10^8$ m^2/s)
50	0.85	1.23
70	2.03	1.88
100	3.42	3.12
150	5.20	3.89

[a] $\sigma_{gg} = 0.7$ Å. [b] $\sigma_{gg} = 0.9$ Å.

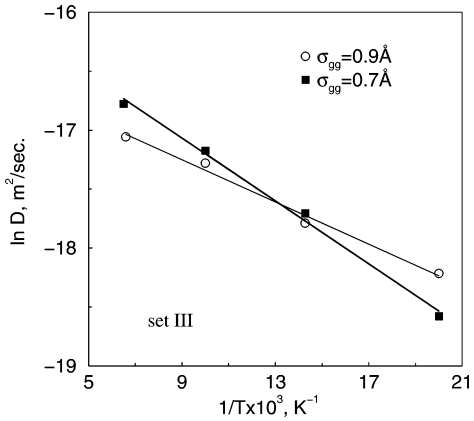

Figure 13. Arrhenius plot of the self-diffusivity, D, for set III at 50 K.

TABLE 4: Friction for Particles in the Linear ($\sigma_{gg} = 0.7$ Å) and Anomalous ($\sigma_{gg} = 0.9$ Å) Regimes at 50 K

set	σ_{gg} (Å)	$\zeta \times 10^{14}$ (kg/s)
I	0.7	9.525
	0.9	5.332
II	0.7	9.277
	0.9	5.612
III	0.7	9.317
	0.9	6.655
IV	0.7	9.124
	0.9	6.632

correlations are seen in the static structure factor, $S(k)$. This probably suggests that the diffusing species has a lower self-diffusivity at around the first and second shells. In contrast, for the low-density high-temperature fluid which Levesque and Verlet investigated,[42] $\Delta\omega(k)/2Dk^2$ decreased monotonically with k. In this case, it appears that the low density does not lead to lowering of the diffusion rate at intermediate k. The spatial

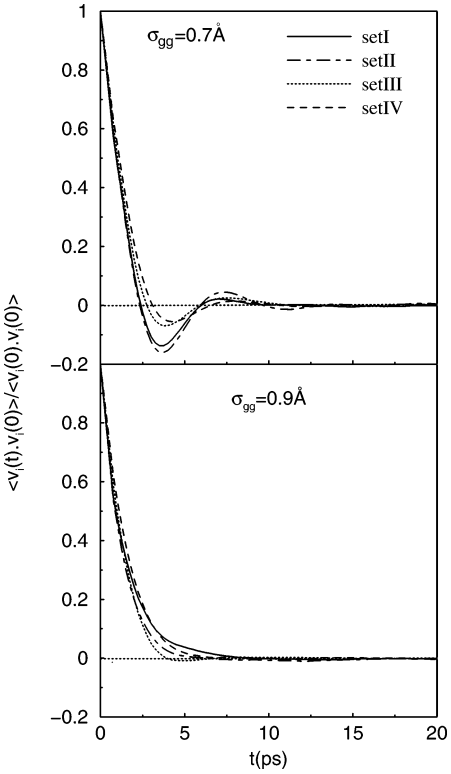

Figure 14. Velocity autocorrelation function for the linear and anomalous regime particle at 50 K.

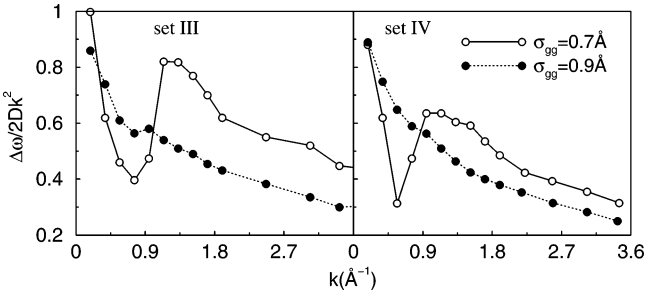

Figure 15. $\Delta\omega(k)/2Dk^2$ as a function of k at 50 K.

correlations are largely weakened at this density, and no well-defined first and second shell of neighbors exist. Thus, the behavior of $\Delta\omega(k)/2Dk^2$ provides interesting insight into rate of diffusion near the first few shells of neighbors.

Figure 15 shows the variation of $\Delta\omega(k)/2Dk^2$ with k for sets III and IV where $\sigma_{gg} = 0.7$ Å (from LR) and $\sigma_{gg} = 0.9$ Å (from AR). For $\sigma_{gg} = 0.7$ Å, a minimum and a maximum are observed as k increases. In contrast, for $\sigma_{gg} = 0.9$ Å, a monotonic decrease with k is observed. Our calculations are at a density of $\rho^* = 0.933$. This is higher than that of Nijboer and Rahman[41] ($\rho^* = 0.8442$), and at such high densities one expects a minimum in $\Delta\omega(k)/2Dk^2$. Thus, the behavior of the particles in LR (for example, $\sigma_{gg} = 0.7$ Å) is understandable. However, the *larger* particles in the anomalous regime (with $\sigma_{gg} = 0.9$ Å) show that it is able to diffuse unimpeded by the spatial correlations even in a *dense* liquid *without* encountering any barrier. This is because of the symmetry encountered by the guest when its size is comparable to the neck diameter. This leads to mutual cancellation of forces exerted by the host on the guest (Figure 1). The behavior of the guest in the anomalous regime approaches that of a free particle. *The dependence of LR is similar to diffusion within a high-density low-temperature fluid, while that of the larger sized particle in AR is similar to diffusion within a low-density high-temperature fluid.* Note that the calculations of both Nijboer and Rahman[41] and Levesque and Verlet[42] are for a single-component fluid consisting of equal-sized Lennard−Jones particles, while ours is for a binary mixture.

Phenomenologically speaking, one could think of $\Delta\omega(k)/2Dk^2$ as a wavelength-dependent diffusion constant, $D(k)$. From Figure 15, it is clear that at large k (~ 3 Å^{-1}) a particle in the linear regime has a higher $\Delta\omega(k)/2Dk^2$ than one in the anomalous regime. Thus, at initial times and short distances, the linear regime has a higher self-diffusivity than the larger particle from the anomalous regime. The minimum $\Delta\omega(k)/2Dk^2$ for the linear regime at intermediate k values is associated with the strong oscillatory component in atomic motion seen in the vacf (Figure 14) which is absent for the anomalous regime. Later, we shall see that this is in agreement with the model of Singwi and Sjölander. As already discussed, in the case of the single-component fluid, previous studies revealed[41,42] that they are associated with spatial correlations; diffusion over distances where spatial correlations exist is less favorable. *Surprisingly, a particle in the anomalous regime appears to be unaffected by these spatial correlations, although, unlike in the low-density fluid, investigated by Levesque and Verlet,[42] strong spatial correlations exist.*

Zeolites Y and A have large cagelike structures (diameter ≈ 11−12 Å) interconnected via narrower windows (7.5 Å in zeolite Y and 4.0 Å in zeolite A). In previous studies on these zeolites with guests of varying sizes, it was found that an energetic barrier is seen for the linear regime.[9] For the anomalous regime, no such barrier is seen at the window, the bottleneck for diffusion.[9] In the present study on dense fluids, the narrow necks that interconnect two voids provide the bottlenecks for diffusion. Thus, the minimum in $\Delta\omega(k)/2Dk^2$ for the linear regime, seen at around 1.0 Å^{-1}, could be caused by the slowdown in the motion of the guest from the energetic barrier associated with its passage through the various shells of the neighbors, probably the first shell of neighbors. For the anomalous regime no such decrease is seen probably because of the absence of any such barrier. A smooth variation in $\Delta\omega(k)/2Dk^2$ with k appears to suggest this. At large k, both the linear regime and anomalous regime vary as $1/k$ with k.[21] Further, as our recent[43] calculations suggest, a particle in LR exhibits a maximum and a minimum in $\Delta\omega(k)/2Dk^2$, while a particle in AR shows a monotonic decrease of $\Delta\omega(k)/2Dk^2$ with k. Thus, the present calculations suggest that the behavior in a dense fluid is, in many ways, similar to the behavior of a diffusant in a porous solid.

3.2.6. Decay of Intermediate Scattering Function. The minimum in $\Delta\delta(k)/2Dk^2$ for the particle in the linear regime and the energetic barrier is likely to lead to well-separated time scales for motion before and after passing the energy barrier, from spatial correlations. Decay of $F_s(k, t)$ at small k will therefore exhibit two distinct time scales since it experiences an inhomogeneous environment. The motion at short times is facile, but at long times, the motion is slowed due to a barrier encountered by the LR particle at the neck. For the particle in the anomalous regime, the absence of such slowing and the absence of any energetic barrier past the first shell are expected to lead to a homogeneous motion at small k, throughout. The signature of these should be seen in density fluctuations.

We have calculated the intermediate scattering function, $F_s(k, t)$, in dense liquids for sets III and IV where $\sigma_{gg} = 0.7$ (LR) and 0.9 Å (AR) particles. Figure 16 shows a plot of $F_s(k, t)$ for

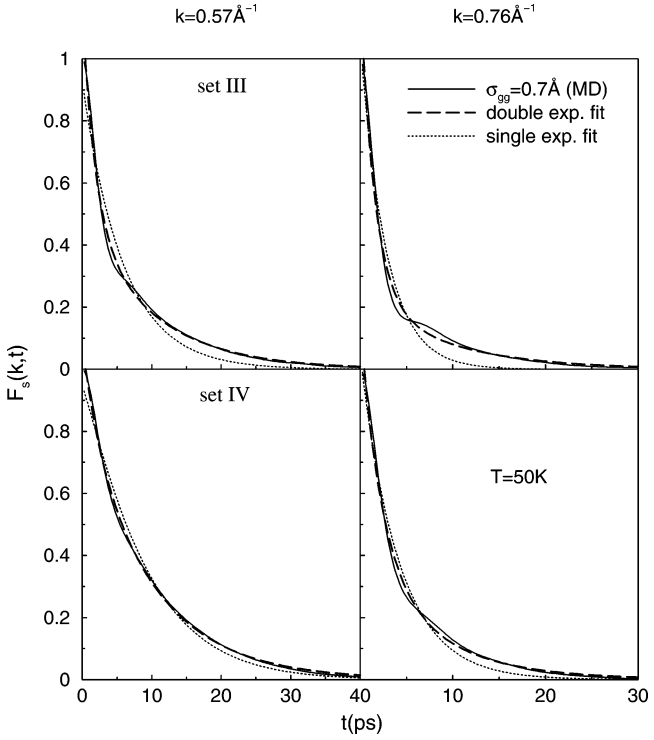

Figure 16. Intermediate scattering function, $F_s(k, t)$, for linear regime particle (σ_{gg} = 0.7 Å) is shown along with a single (e^{-t/τ_1}) and a biexponential ($e^{-t/\tau_1} + e^{-t/\tau_2}$) fit.

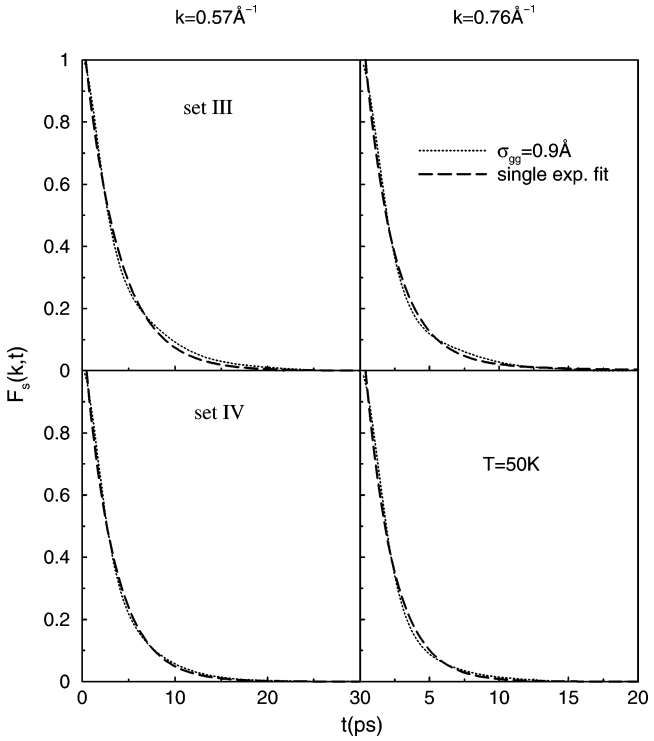

Figure 17. Intermediate scattering function, $F_s(k, t)$, for anomalous regime particle (σ_{gg} = 0.9 Å) is shown along with a single (e^{-t/τ_1}) exponential fit.

0.7 Å, and Figure 17 shows it for 0.9 Å and for $k = 0.57$ and 0.76 Å^{-1}. We have fitted a single (e^{-t/τ_1}) and a double exponential ($e^{-t/\tau_1} + e^{-t/\tau_2}$) to $F_s(k, t)$ at $k = 0.57$ and 0.76 Å^{-1}. The values of τ_1 for the particle in AR and τ_1 and τ_2 for the LR are listed in Table 5. A single-exponential decay provides a good fit to the $F_s(k, t)$ (see Figure 17) for the 0.9 Å particle but

TABLE 5: Values of τ_1 for the Particle in the Anomalous Regime and τ_1 and τ_2 for the Particle in the Linear Regime for Sets III and IV

	$\sigma_{gg} = 0.7$ Å				$\sigma_{gg} = 0.9$ Å	
	$k = 0.57$ Å^{-1}		$k = 0.76$ Å^{-1}		$k = 0.57$ Å^{-1}	$k = 0.76$ Å^{-1}
set	τ_1	τ_2	τ_1	τ_2	τ_1	τ_1
III	1.84	9.09	1.01	4.13	3.71	2.23
IV	1.15	4.60	1.32	2.50	3.17	2.01

not for the 0.7 Å particle (see Figure 16). For the latter, a double exponential provides a good fit. This is consistent with the behavior of $\Delta\omega(k)/2Dk^2$.

3.2.7. Physical Picture of Solute Motion. The picture that emerges for motion of a solute among the solvent is as follows: A particle in the linear regime diffuses in a facile manner up to a short distance, a distance probably determined by the first shell of solvent neighbors. Diffusion past this first shell of neighbors is not facile. The particle from LR encounters a distinct energy barrier at the first shell of neighbors. Both the potential energy barrier and entropic barrier are expected at the first shell. Once the particle in LR manages to overcome this barrier and moves past the first shell of solvent neighbors, the solute diffuses over a relatively larger distance without difficulty. Relaxation time τ_1 is associated with the motion within the first shell. Relaxation time τ_2 is associated with motion past the first shell. The particle from LR probably performs such motion alternately. This scenario is similar to the model of Singwi and Sjölander.[44] Singwi and Sjölander proposed their model to describe the motion of solute in liquid water. Because of the extensive hydrogen bonding in water, the motion of water molecules relative to that of solute is slow. This is also the case in the present study.

We propose that the maximum at larger k corresponds to the motion of the particle within the "cage" formed by the first shell of neighbors in the liquid. When the cage does not exist, the vacf shows no oscillations and motion is not separated into motion within and without the cage. This is true at the low-density high-temperature phase of a fluid. It is only when the fluid is at high density and low temperature that motion has two well-defined regimes, motion within the cage formed by the first shell of neighbors (small k) and motion outside of it (intermediate k). This separation is possible since at high densities and low temperatures, the atom encounters a distinct barrier during its passage through the first few shells of neighbors.

The picture that emerges for the motion of a particle in AR is completely different from that of a particle in LR. This is the first time that existence of an anomalous regime in dense fluids has been noted. Therefore, there are no previous models to describe the nature of motion of a particle in the anomalous regime. A particle in AR, unlike a particle in LR, does not encounter a barrier at the first shell of solvent molecules. As a consequence, the two distinct types of motion, one within the first shell of neighbors and the other outside the first shell of neighbors, are not seen. Therefore, two distinct relaxation times do not exist. In other words, a particle in AR experiences or "sees" a homogeneous solvent environment.

A particle in LR probably performs an oscillatory motion inside the first shell of neighbors before escaping from it. Thus, the first shell provides a cagelike structure in which the solute is trapped for a period. A particle in AR has no cagelike structure to trap it.

It is interesting to see if there are any real systems in which the above situations can be realized. It is possible to choose

binary mixtures of nearly spherical atoms or molecules with an appropriate diameter for the two components. Instead of varying the diameter of the guest, we could alter the density or pressure of the binary mixtures. This will, in turn, vary the void and neck dimensions, and the diffusivity maximum might be seen at the appropriate density. We have investigated ion conductivity of alkali and halide ions in polar solvents. We found a maximum for the self-diffusivity of an ion at an appropriate size. This provides an example of a real, dense system which exhibits LE.

Further, a comparison of the results of Nijboer and Rahman and those of Levesque and Verlet suggests that particles, typically at higher densities, exhibit a minimum in $\Delta\omega(k)/2Dk^2$ at some intermediate k value. The minimum does not exist at low densities and high temperatures. This study reveals that *even at high density, a particle in the AR exhibits no such minimum in* $\Delta\omega(k)/2Dk^2$*, although a smaller particle from the LR exhibits a minimum*. This is counterintuitive and comes from LE. It is probably caused by the absence of an energetic barrier for AR during its passage through the first shell of neighbors of the host/solvent particles.

3.2.8. Model of Singwi and Sjölander. The model proposed by Singwi and Sjölander[44] seems to be appropriate for a particle in the linear regime. Their model suggests that a particle performs an oscillatory motion for a period τ_1 before performing diffusive motion with a characteristic time τ_2. The particle alternates between oscillatory and diffusive motion. This model leads to the biexponential decay of $F_s(k, t)$ and appears to be appropriate for the motion of the particle in the linear regime. Here, oscillatory motion arises from bottlenecks to diffusion experienced by the linear regime particle at the necks separating two voids. This picture, however, is not valid for a particle in the anomalous regime which encounters relatively more homogeneous potential energy landscape and no barrier at the necks separating neighboring voids.

4. Conclusions

The results show an enhancement in the self-diffusivity of the guest particles for a characteristic size related to the diameter of the void space of the host fluid. This is analogous to the *levitation effect* observed previously for particle diffusion in porous solids. Calculations of the wavevector dependence of the full width at the half-maximum (fwhm), $\Delta\omega(k)$, of the self-part of the dynamic structure factor for linear and anomalous regime show a minimum in $\omega(k)$ at a value of k corresponding to the first shell neighbor for the particle in the linear regime. For the anomalous regime no such minimum is seen. This suggests that the particle in the linear regime encounters a barrier to diffusion at distances where strong spatial correlations exist.

These results suggest that diffusion within liquids may strongly depend on the size of the diffusing species. Many of the processes occurring in liquid medium, such as chemical reactions or diffusion of electrolytes, will need to be reconsidered in light of these results. These results have implications in biological processes too. The fact that the anomalous maximum in self-diffusivity exists even in a liquid host (apart from well-ordered solids) means that levitation effect (or anomalous maximum) may exist in amorphous solids and glasses as well.

It is not clear from the above discussions when the Stokes−Einstein law is valid and when there is a breakdown in the Stokes−Einstein relationship. For a solute, such as a polymer diffusing in a solvent of a relatively smaller size, the Stokes−Einstein relationship, $D = kT/4\pi\eta a$, is valid. Here, the size of the solute molecule is large and the size of the solvent molecule relative to that of the solute is small. This study suggests that the Stokes−Einstein relation is not valid for systems in which the solute is smaller than the solvent.

Two distinct regimes exist when the solute is smaller than the solvent. When $a_{solute} \ll a_{solvent}$, where a refers to the radius, the self-diffusivity of the solute lies in the linear regime of LE. As the size of a_{solute} increases and approaches that of the void then an anomalous maximum in diffusivity is observed. This situation is realized for $a_{solute} \approx \beta a_{solvent}$, where $\beta = 0.155$ (for fcc lattice) or 0.20−0.25 (for liquid). The present study suggests that the relevant quantity for determining if there will be a breakdown of the Stokes−Einstein relationship is not the size of the solute alone. Instead, the important quantity for determining if there will be a breakdown of the Stokes−Einstein law is the dimensionless quantity $\alpha = a_{solute}/a_{solvent}$. For $1 \leq \alpha < \infty$, the Stokes−Einstein law is valid. For $0.25 < \alpha < 1.0$, the Stokes−Einstein law is probably still valid. The anomalous regime of LE is found near $\alpha = 0.25$. For $\alpha < 0.20$ the linear regime or $D \propto 1/\sigma^2$ is valid. Note that the value of β can be quite different when interactions other than van der Waals interactions dominate.

The comparison of LE in dense fluids with LE in porous solids is worth noting. The diffusivity maximum or *levitation effect* is seen in dense liquids even at the relatively higher temperature of $T^* = 1.663$. In the case of guests in zeolites, previous studies[36] have shown that the LE exists only at relatively low temperatures. Although it is difficult to make a direct comparison since the two systems are quite different, the existence of a diffusion maximum at $T^* = 1.663$ suggests that LE is likely to be more common in dense liquids. It also suggests that LE is not so *fragile*. That is, LE might persist at quite high temperatures. In fact, a comparison with the previous work of Yashonath and Chitra[36] suggests that the height of the diffusivity maximum is probably more significant in dense liquids than in porous solids and they persist at higher temperatures in dense liquids than in porous solids.

We shall discuss elsewhere the role of LE in determining the ionic conductivity of polar solvents.

Acknowledgment. We gratefully acknowledge the financial support from the Department of Science and Technology, New Delhi.

References and Notes

(1) Bhide, S. Y.; Yashonath, S. *J. Chem. Phys.* **2002**, *116*, 2175.
(2) Bhide, S. Y.; Yashonath, S. *J. Phys. Chem. B* **2000**, *104*, 11977.
(3) Bhide, S. Y.; Yashonath, S. *J. Phys. Chem. A* **2002**, *106*, 7130.
(4) Bhide, S. Y.; Yashonath, S. *J. Am. Chem. Soc.* **2003**, *125*, 7425.
(5) Levitt, D. *J. Phys. Rev. A* **1973**, *8*, 3050.
(6) Fedders, P. A.; Sanky, O. F. *Phys. Rev. B* **1977**, *15*, 3580.
(7) Kärger, J.; Ruthven, D. M. *Diffusion in zeolites and other microporous solids*; North Publications: New York, 1985.
(8) Bhide, S. Y.; Yashonath, S. *J. Chem. Phys.* **1999**, *111*, 1568.
(9) Yashonath, S.; Santikary, P. *J. Phys. Chem.* **1994**, *98*, 6368.
(10) Bandyopadhyay, S.; Yashonath, S. *J. Phys. Chem.* **1995**, *99*, 4268.
(11) Kumar, A.; Yashonath, S. *J. Phys. Chem. B* **2000**, 104, 9126.
(12) Azaroff, L. V. *Introduction to Solids*; Tata McGraw-Hill: New Delhi, India, 1990.
(13) Atkins, P. W. *Physical Chemistry*; Oxford University Press: Oxford, U.K., 1986.
(14) Bagchi, B.; Biswas, R. *Acc. Chem. Res.* **1998**, *31*, 181.
(15) Zwanzig, R. *J. Chem. Phys.* **1970**, *52*, 3625.
(16) Wolynes, P. G. *J. Chem. Phys.* **1978**, *68*, 473.
(17) Koneshan, S.; Lynden-Bell, R. M.; Rasaiah, J. C. *J. Am. Chem. Soc.* **1998**, *120*, 12041.
(18) Chowdhuri, S.; Chandra, A. *Proc. − Indian Acad. Sci., Chem. Sci.* **2001**, *113*, 591.
(19) Chowdhuri, S.; Chandra, A. *Phys. Rev. E* **2002**, *66*, 041203.
(20) Starr, F. W. J. N.; Stanley, H. *Phys. Rev. Lett.* **1999**, *82*, 2294.
(21) Boon, J. P.; Yip, S. *Molecular Hydrodynamics*; Dover: New York, 1980.

(22) Urakawa, A.; Wirz, R.; Burgi, T.; Baiker, A. *J. Phys. Chem. B* **2003**, *107*, 13061.
(23) Morales-Cabrera, M. A.; Perez-Cisneros E. S.; Ochoa-Tapia, J. A. *Ind. Eng. Chem. Res.* **2002**, *41*, 4626.
(24) Parrinello, M.; Rahman, A.; Vashistha, P. *Phys. Rev. Lett.* **1983**, *50*, 1073.
(25) Vashistha, P.; Rahman, A. *Phys. Rev. Lett.* **1978**, *40*, 1337.
(26) Allen, M. P.; Tildesley, D. J. *Computer Simulation of Liquids*; Clarendon Press: Oxford, U.K., 1987.
(27) Corti, D. S.; Debenedetti, P. G.; Sastry, S.; Stillinger, F. H. *Phys. Rev. E* **1997**, *55*, 5522.
(28) Sastry, S.; Corti, D. S.; Debenedetti, P. G.; Stillinger, F. H. *Phys. Rev. E* **1997**, *56*, 5524.
(29) Weissberg, H. L.; Prager, S. *Phys. Fluids* **1962**, *5*, 1390.
(30) Shahinpoor, M. *Powder Technol.* **1980**, *25*, 163.
(31) Tanemura, M.; Ogawa, T.; Ogita, N. *J. Comput. Phys.* **1983**, *51*, 191.
(32) Kumar, A. V. A.; Yashonath, S. *J. Phys. Chem. B* **2000**, *104*, 9126.
(33) Maitland, G. C.; Rigby, M. E. B. S. W. W. *Intermolecular Forces: Their Origin and Determination*; Clarendon Press: Oxford, U.K. 1981.
(34) Laidler, K. J.; Meiser, J. H. *Physical Chemistry*; Benjamin-Cummings: Reading, MA, 1982.
(35) Finney, J. L.; Wallace, J. *J. Non-Cryst. Solids* **1981**, *43*, 165.
(36) Yashonath, S.; Rajappa, C. *Faraday Discuss.* **1997**, *106*, 105.
(37) Rajappa, C.; Yashonath, S. *Mol. Phys.* **2000**, *98*, 657.
(38) Rajappa, C.; Yashonath, S. *J. Chem. Phys.* **1999**, *110*, 5960.
(39) Ghorai, P. K.; Yashonath, S.; Demontis, P.; Suffritti, G. B. *J. Am. Chem. Soc.* **2003**, *125*, 7116.
(40) Herwig, K. W.; Wu, Z.; Dai, P.; Taub, H.; Hansen, F. Y. *J. Chem. Phys.* **1997**, *107*, 5186.
(41) Nijboer, B. R. A.; Rahman, A. *Physica* **1966**, *32*, 415.
(42) Levesque, D.; Verlet, L. *Phys. Rev. A* **1970**, *2*, 2514.
(43) Ghorai, P. K.; Yashonath, S. *J. Phys. Chem. B* **2005**, in press.
(44) Singwi, K. S.; Sjölander, A. *Phys. Rev.* **1960**, *119*, 863.